Transport properties of polyaniline-cellulose-acetate blends

Jérôme Planès,* Andreas Wolter, Yasmina Cheguettine, Adam Proń, Françoise Genoud, and Maxime Nechtschein
Laboratoire de Physique des Métaux Synthétiques, UMR 5819 CEA–CNRS–Université Joseph Fourier, Département de Recherche Fondamentale sur la Matière Condensée, CEA-Grenoble, 17 rue des Martyrs, F-38054 Grenoble, Cedex 9, France
(Received 26 February 1998)

Transport properties of polyaniline (PANI)–cellulose acetate (CA) conducting blends have been investigated at various length scales and temperatures. We report on the results of dc and ac conductivity measurements, magnetoresistance and electron-spin resonance (ESR) performed on composite films with PANI weight fraction p ranging from the percolation threshold—$p_c \simeq 0.1\%$—to a few percent. Three different PANI doping agents have been tested, namely, camphor sulfonic acid (CSA), di(i-octyl phosphate) (DiOP) and phenyl phosphonic acid (PPA). The percolative behavior of σ_{dc} resembles that of published results on PANI/PMMA blends. The onset frequency ω_ξ of the dispersion in σ_{ac} appears to follow the scaling law: $\omega_\xi \propto \sigma_{\mathrm{dc}}^z$ with $z \simeq 1$. The temperature dependence is of the form of $\ln\sigma(T) \propto -(T_0/T)^\gamma$ the exponent decreasing from 0.75 to 0.5 with increasing p. The microscopic metallic character of transport is found in ESR and microwave measurements. Spin-dependent conductivity is inferred from the $(B/T)^2$ universal behavior of magnetoresistance. Those results are discussed in conjunction with the ongoing debate on the nature of disorder in conducting polymers—homogeneous versus heterogeneous. [S0163-1829(98)01235-1]

I. INTRODUCTION

The processability of doped polyaniline (PANI) in m-cresol was discovered[1] in 1992 and has led to a somewhat ''new polyaniline'' with enhanced conductivity ($\sigma \geqslant 300$ S cm^{-1} at room temperature) and metallic behavior [positive temperature coefficient of resistivity at approximately room temperature (RT)]. Numerous studies are devoted today to the disorder-induced metal-insulator transition in this conducting polymer (CP).[2–4] Disorder is indeed the leading parameter of transport properties and it is in turn dramatically influenced by processing conditions.[5]

One way to influence the structural disorder at a supramolecular scale is to mix the CP with an insulating polymer in a cosolvent.[6,7] m-cresol is able to dissolve many traditional polymers among which the widespread cellulose acetate (CA). Note that the ''PANI solution'' might be an improper description,[8,9] but at least a satisfactorily low degree of aggregation in the dispersion is reached. It shall be a necessary condition to get a conduction threshold as low as 10^{-3} in weight fraction of PANI.

The purpose of this paper is to investigate transport properties of conducting films of PANI blended with CA. Attention has been paid probing a large range of length scales. Macroscopically, the percolative behavior of static conductivity shows that long-range correlations of the so-called PANI network do influence electronic transport. At the other end, the independence of microscopic conductivity versus concentration, as probed by ESR, gives evidence that local properties of PANI chains (or fibrils) are retained in blends.

Marks of disorder are found in the variation of conductivity versus temperature and frequency. The thermal behavior is correctly described by generalized hopping models, but the exponent γ is concentration dependent and greater than $\frac{1}{2}$. This fact has been attributed to superlocalization within variable range hopping (VRH) theory elsewhere.[6] A careful analysis of granular conduction models provides another scheme to account for those values for γ.[10,11]

The paper is organized as follows: Sec. II describes sample preparation and techniques; Sec. III presents and discusses the results of measurements of conductivity as a function of PANI contents, of temperature, of magnetic field, of frequency and finally gives ESR data; Sec. IV contains a general discussion and sums up the findings of the present study.

II. EXPERIMENT

A. Sample preparation

The preparation of the composite films used throughout this study has been reported in detail in Ref. 7. A summary follows. Polyemeraldine base with relatively high molecular weight[12] ($M_n = 21\,500$ and $M_w = 71\,000$ g/mol) is mixed with one of the protonating agents: camphor sulphonic acid (CSA), phenyl phosphonic acid (PPA), or dioctyl phosphate (DiOP), at 0.5 molar ratio of dopant molecule to PANI repeat unit. From the suspension of this mixture in m-cresol at 0.5 wt % PANI content, the so-called soluble part (after centrifugation) is extracted and its concentration determined. This solution is mixed in various ratios with a 5 wt % m-cresol solution of CA and the plasticizers. Solutions are subsequently cast onto a glass plate and the solvent slowly evaporated at temperatures of 50–60 °C, yielding highly flexible and transparent films. Their thickness ranges from 20 to 80 μm. Thicker films are obtained for lower PANI content, because the viscosity of the solution is higher and the spreading of the drop is not limited by walls.

It has been checked that the UV-vis-NIR spectra of the PANI solution and the solid films were quite similar, exhibiting strong absorbance at long wavelengths together with a small polaron peak in the 800–900 nm region.[7] It proves that (i) PPA and DOP confer to PANI (in m-cresol solution) the same qualitative conformation, responsible for some delocalization of the polaronic species, as that already known for CSA,[1] (ii) the conformation is retained during the evaporation process. A significant amount of m-cresol also remains.

For some specific ac-conductivity measurements a metallic substrate was substituted for the glass plate. With steel, the solution reacts chemically: oxidation traces are visible on the substrate after the film has been peeled off and the adhesive force is strong. This effect is also visible indirectly in the conductivity value. In a sandwich-type measurement, very sensitive to any ''insulating'' layer, the apparent conductivity is reduced by 1 or 2 orders of magnitude, compared to that of the films evaporated on glass. Conversely, no discrepancy is observed in the longitudinal measurement (as the standard four-probe) for which the bulk resistance is dominant because of the probes spacing being much larger than the film thickness. The capacitative effect is also observed in ac-conductivity. If, however, the substrate is gold plated, these effects vanish. The data presented and discussed in Secs. III D and III E correspond to glass substrates.

B. dc conductivity and magnetoresistance measurements

RT conductivity values have been obtained by the four-probe method. The temperature dependence of the conductivity was also measured by a four-contact device. Four parallel gold wires of 0.1 mm diameter are pressed onto one face of the rectangular sample. The voltage probes are 4 mm apart. To eliminate voltage offsets, conductivity was always measured for both polarities of the current and linearity was checked for each point. The current was supplied by a Keithley Model 220, the potential of the two voltage contacts was measured independently by two electrometers (Keithley Model 6512, input impedance $\geqslant 2.10^{14}\ \Omega$). The probe head was placed into a Oxford CF1200D continuous flow cryostat permitting operation between 5 and 300 K. Sample temperature was measured by a rhodium-iron resistance thermometer and regulated with an Oxford ITC503 controller.

Magnetoresistance experiments were performed in the magnetic field provided by a Oxford superconducting coil. The field reaches 11.5 T and the sample can be cooled down to 1.4 K by pumping over the helium bath. Below 4.2 K the regulation was made by the equilibrium gas pressure. The temperature sensor was a Cernox, almost insensitive to the magnetic field. The probe head was identical to that of dc conductivity, except that it could be rotated in the plane of the film for the field to be parallel or perpendicular to the electric current. The signal-to-noise ratio is optimized by taking the highest value of current from the linear part of the $V-I$ characteristics. At very low temperatures, the sample heating is prevented by limiting the input power to less than $1\ \mu$W.

C. ac-conductivity measurements

The complex conductivity (or permittivity) was measured between 10 Hz and 18 GHz on the same sample using an impedance meter HP4192A and two vectorial network analyzers HP4191A and Wiltron 37241A. A 7-mm-diam disk is punched out of the polymer film and inserted at the end of a coaxial line (APC7 standard) before the short. Electrical contacts are ensured by gold evaporation on each side of the sample; for the side of the inner conductor, gold is deposited only at the center of the sample in a 3-mm-diam disk. At low frequency ($\nu \leqslant 1$ GHz) and small thickness ($d \leqslant 0.5$ mm) this setup is equivalent to a capacitance measurement; the conductivity is extracted from the admittance or the reflection coefficient by the Marcuvitz approximation.[13] In other cases the propagation of the electromagnetic wave in the sample has to be considered and Maxwell's equations solved for this geometry.[14] Low-temperature measurements are performed in an Oxford CF1200D continuous-flow cryostat. Electromagnetic waves propagate in a rigid, airtight, steel coaxial line with characteristic impedance $50\ \Omega$ up to 20 GHz, designed by Alpen. A one-point temperature dependent calibration is added to the standard RT short-open-load in order to take into account the influence of low temperature on the electrical characteristics of the line: reduced losses and phase rotation. A rhodium-iron resistance thermometer is placed as close as possible to the measurement cell. Two cells have been designed that are—at least partly—made of brass for a better thermal contact with the sample.

D. Electron spin resonance

The ESR experiments have been performed with an ER 200 Bruker ESR X band spectrometer. The sample in a quartz tube was placed inside the cavity and connected to a pumping line. The ESR linewidth (the full linewidth at half-maximum, $\Delta H_{1/2}$, and the peak-to-peak linewidth, ΔH_{pp}) could be recorded at various temperatures.

III. RESULTS

A. Percolation at room temperature

One of the most striking effects in conducting blends made by the codissolution process described in Sec. II A is the percolative behavior of the conductivity as a function of the PANI weight fraction. It is illustrated in Fig. 1 for two dopants: PPA and DiOP. Table I sums up the fitting parameters p_c and t of the scaling law $\sigma(p)=\sigma_0(p-p_c)^t$ for different preparations. The lowest percolation threshold $p_c = 0.067\%$ is obtained for the PPA dopant; but PANI(PPA) is the least conducting of the three preparations. Some variability is to be noted in the data of *a priori* identical samples: in fact, this reveals the crucial role of processing. For blends prepared with unplasticized cellulose acetate, the conduction threshold is, however, approximately 10 times higher.[7]

Comparable results have been obtained with PMMA as a matrix and the CSA dopant.[6] In Ref. 6, the threshold is assumed to be $p_c = 0.3\%$ despite the continuously gentle decrease of $\sigma(p)$ for $p \leqslant p_c$. Similarly, low thresholds were also observed with gels,[15] blends of conducting polymer nanoparticules,[16] and carbon black composites.[17] Because their mixings seem to conduct at arbitrary low load content, some authors prefer to exclude the percolation mechanism. In our case, a real threshold is observed also in the low-frequency dielectric constant: Fig. 2 shows for PANI(DiOP)/CA, for which $p_c \simeq 0.5-0.6\%$, that ε' and ε'' are low and constant for $p \leqslant 0.4\%$, diverging at vanishing frequency for $p \geqslant 0.7\%$ and intermediate for $p = 0.5$and $p = 0.6\%$.

In each case, the key point is thought to lie on particular aggregation processes yielding a loose network for the charge carriers to proceed. According to transmission-electron-microscopy (TEM) observations,[6,18] the solution blending process (this work and Ref. 6) also results in a self-assembling network derived from the liquid-liquid phase

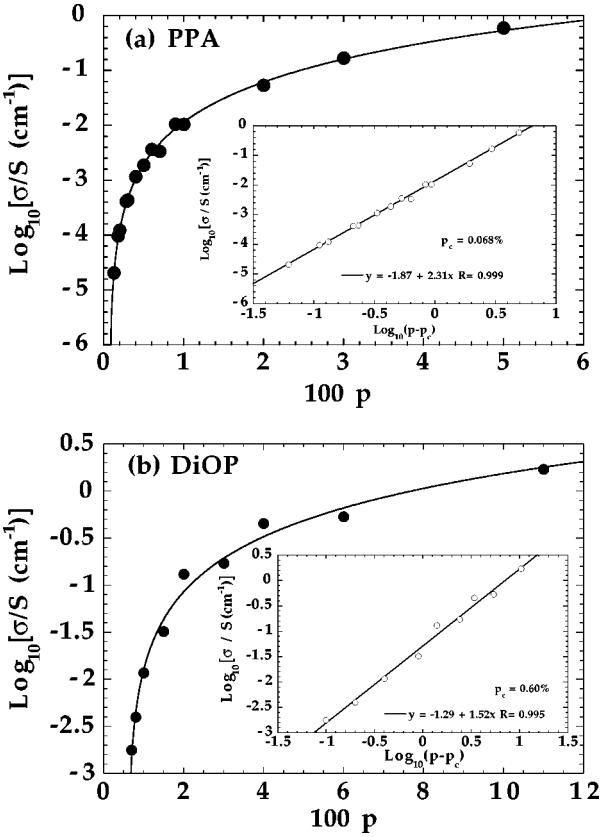

FIG. 1. Conductivity σ vs weight fraction p of PANI in CA for two polyaniline dopants: (a) Phenyl phosphonic acid; (b) dioctyl phosphate. Insets show the percolation scaling law between σ and $p-p_c$ for $p \geqslant p_c$.

separation. Because the TEM sample preparation conditions are rather severe—dissolution of the host matrix while keeping the tenuous structure of PANI — those images have to be carefully interpreted but they remain the only ones available to date and therefore deserve attention.

These systems unfortunately seem quite far from model systems studied in the flourishing literature on (classical) polymer blends; they are multicomponent (PANI, dopant, host matrix, residual solvent, ''compatibilizers''), diluted, i.e., highly nonsymmetric, and may involve special type of polymer-polymer interactions due to the conjugated nature of PANI. A thermodynamic study thus remains a challenge but would provide clues for questions such as how to reduce variability between preparations or whether there is an ultimate threshold, and for what molecular weight of the components. Equilibrium thermodynamics has already been put

TABLE I. Percolation threshold p_c and scaling exponent t for different series of PANI/CA blends.

Sample	p_c	t
PANI(CSA)/CA first series	0.85%	2.9 ± 0.3
PANI(CSA)/CA second series	$\leqslant 0.1\%$	1.8 ± 0.1
PANI(DiOP)/CA first series	0.4%	2.3 ± 0.1
PANI(DiOP)/CA second series	0.6%	1.5 ± 0.1
PANI(PPA)/CA first series	0.26%	2.3 ± 0.1
PANI(PPA)/CA second series	0.07%	2.2 ± 0.1

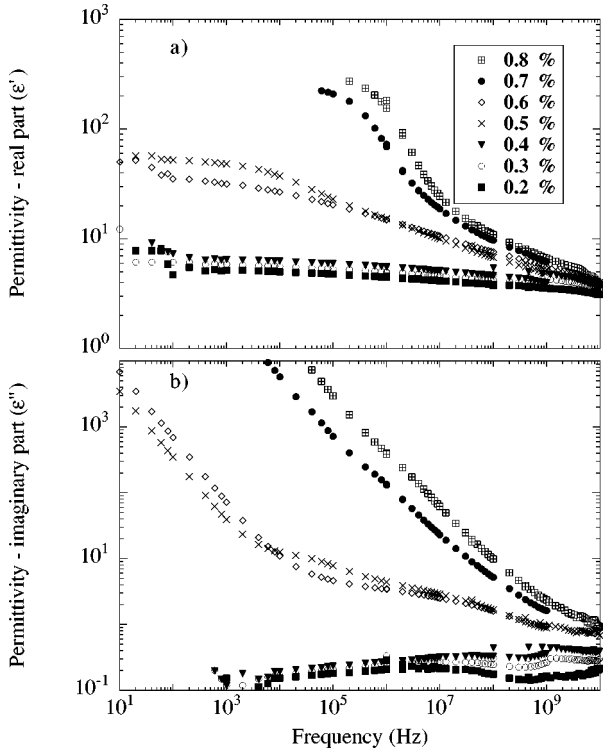

FIG. 2. Complex permittivity of PANI(DiOP)/CA blends for compositions p around p_c: (a) real part; (b) imaginary part.

forward in the context of ''multiple percolation.''[19] In this scheme, the conducting polymer percolates inside the CP-rich phase, itself percolating in the sample. Depending on the coexistence curve, the CP concentration in the rich phase could reach the 16% value characteristic of the percolation of disordered isotropic objects.[20] Ultralow thresholds, however, demand a very peculiar shape — strongly asymmetrical — of the coexistence curve. Finally, it has also been mentionned that viscoelastic phase separation[21,22] naturally yields a metastable network domain structure; instead of a globular shape due to the surface tension driving forces, the viscoelastic stress (meta)stabilizes an anisotropic interface and the minority phase develops elongated and connected structures.

B. *T*-dependent dc conductivity

The temperature dependence of σ_{dc} for PANI(CSA)/CA blends is shown in Fig. 3. All of the curves have been fitted according to

$$\sigma(T) = \sigma_0 \exp\left[-\left(\frac{T_0}{T}\right)^{\gamma}\right], \tag{1}$$

which accounts for hopping conductivity in disordered systems. The fitting parameters γ and T_0 are obtained as follows: γ is the linear slope of $\ln W$ versus $\ln T$, where

$$W = \frac{d \ln \sigma}{d \ln T}.$$

T_0 is extracted from the linear slope of $\ln\sigma$ versus $T^{-\gamma}$ (which is T_0^{γ}). The quality of these fits can be checked in Fig. 4. Slight deviations are sometimes observed in $\ln W$ versus $\ln T$ plots at $T \geqslant 250$ K.

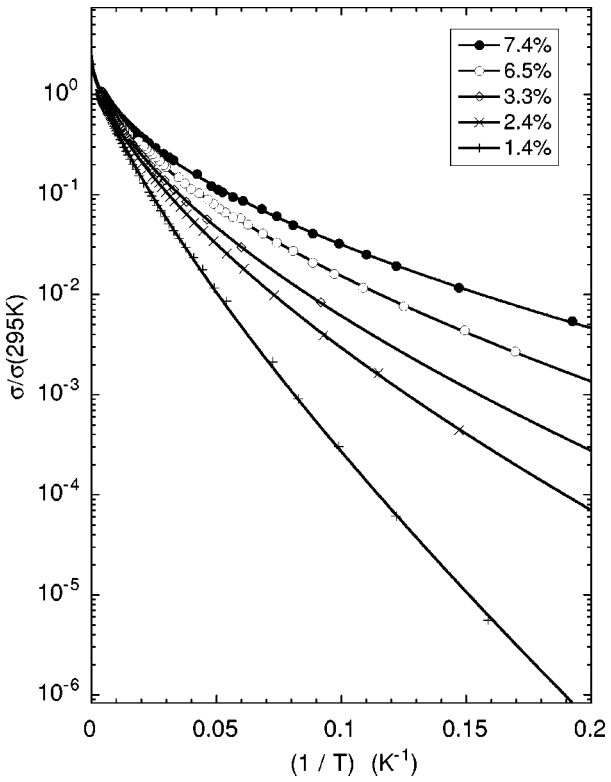

FIG. 3. Reduced conductivity $\sigma(T)/\sigma(295\ \mathrm{K})$ plotted vs inverse temperature for various compositions of PANI(CSA)/CA blends. Lines are fits to Eq. (1) obtained as explained in the text.

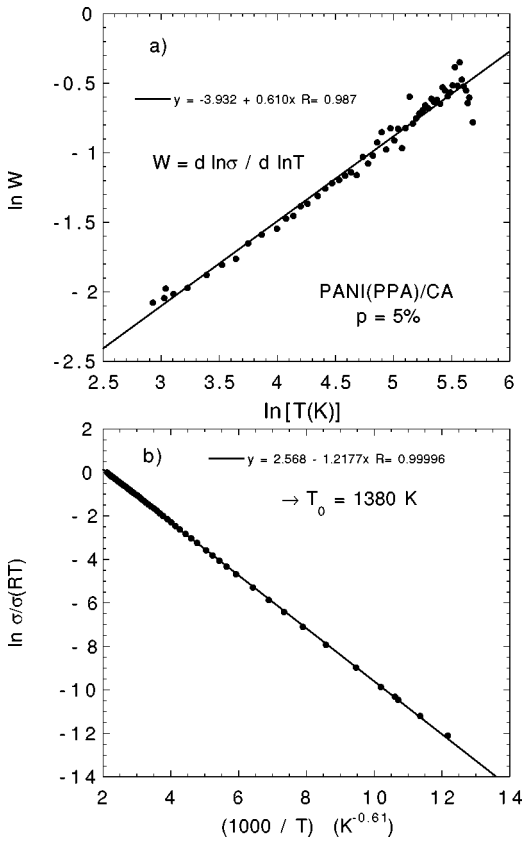

FIG. 4. Illustration of the fitting procedure for $\sigma(T)$: (a) log-log plot of the logarithmic derivative W vs T; (b) plot of $\ln\sigma/\sigma_0$ vs $T^{-\gamma}$.

For the three PANI dopants and for various PANI contents, the fitted parameters are given in Table II. They all follow the general trend: γ increases from 0.5 to 0.8 upon dilution, and T_0 is roughly insensitive to p. A similar behavior has been described by Reghu *et al.*[6] Note, however, that some hierarchy can be drawn: the conductivity of ''pure'' unblended PANI is the highest for the CSA dopant, then for DiOP and the lowest for PPA; correspondingly, typical values for T_0 in the blends are the lowest for CSA, intermediate for DiOP, and the highest for PPA.

In the case of carbon black (C.B.) composites,[17] a constant $\gamma=0.66$ was attributed to superlocalization of wave functions on the C.B. fractal network.[23] This exponent is found for 3d-VRH in the presence of a parabolic gap at ϵ_F on the percolation cluster.

In our case we are looking for the origin of the variation of γ with p. The 0.5 value of the sample with the highest content of PANI is similar to numerous observations in disordered CP. It has been shown[24] that the granular metal model of Sheng adapted to CP by Zuppiroli *et al.*[25] can account well for this behavior. It states that the local transition rate (or conductance) results from the competition between intergrain tunneling and some ''charging'' energy of the grains, where the granularity is related to doping heterogeneities. In this model, the value of T_0 contains the geometrical parameters of the system, namely the size and distance between the grains, and the Coulombic interaction energy. The value of γ is shown to depend on the distribution of grain size. Using the critical-path method, Sheng and Klafter[26] show that $\gamma=0.5$ for a wide range of intermediate temperatures and that a crossover to $0.5\leqslant\gamma\leqslant1$ appears at some higher T. An effective medium treatment of the same model[10,11] also yields the conclusion that $\gamma=0.5$ is submitted to conditions on the distributions; more precisely, one should consider only the ''efficient'' part of the available conductances, i.e., the maximum values of intergrain hopping distance and charging energy are T dependent. Moreover, the actual energy of the grains contains a random part in addition to the charging part proportionnal to the size. This accounts for fluctuations with size and shape of energy levels in small grains.[27,28] Relaxing some of those conditions leads to γ values in the range $0.5-1$. As a matter of fact, the real influence of electronic interactions is still a major question.[29] In granular system, the potential disorder has to be large enough to yield $\gamma=0.5$; in such a case this is the long-range part of Coulomb interaction (between charged grains) that enters the transition rate, and not the on-site (Hubbard) part.

Finally, we have also tried to impose the $\exp(-T^{-1/2})$ dependence at the expense of a (smaller) T dependence of the pre-exponential factor. It actually corresponds to the complete VRH formulation.[30] The fitting function is thus

$$\sigma(T)=\sigma_0\left(\frac{T_0}{T}\right)^q\exp\left[-\left(\frac{T_0}{T}\right)^{\frac{1}{2}}\right]. \tag{2}$$

Because the exponential term is strongly varying, it is expected that changing from γ as given in Table II to $\gamma=\frac{1}{2}$ would dramatically modify T_0. As a matter of fact, we may correctly fit Eq. (2) to our data (see Fig. 5) with the general observation that T_0 rapidly increases for $p\rightarrow p_c^+$ as well as q.

TABLE II. Fitting parameters to Eq. (1) for the thermal evolution of conductivity in different series of PANI/CA blends.

Dopant	100p	σ(RT)/S cm^{-1}	σ_0/S cm^{-1}	γ	T_0/K
CSA first series	7.4	2.4	5.57	0.51	160
	6.5	1.0	2.22	0.55	160
	3.3	$5.5\ 10^{-2}$	0.15	0.54	225
	2.4	$2.0\ 10^{-2}$	0.046	0.61	190
	1.4	$1.8\ 10^{-3}$	0.005	0.71	255
DiOP first series	6.0	1.29	8.0	0.54	810
	4.0	$2.7\ 10^{-1}$	1.14	0.63	450
	1.0	$4.6\ 10^{-2}$	0.14	0.76	300
	0.6	$4.5\ 10^{-4}$	0.0014	0.79	340
DiOP second series	3.9	$2.0\ 10^{-1}$	1.3	0.60	690
	1.0	$5.3\ 10^{-3}$	0.02	0.70	370
PPA first series	10	0.13	9.3	0.54	3100
	6.0	$5.3\ 10^{-2}$	2.1	0.58	2120
	3.0	$1.5\ 10^{-2}$	0.34	0.64	1670
	1.0	$1.0\ 10^{-3}$	0.027	0.67	1780
	0.7	$4.0\ 10^{-4}$	0.01	0.69	1570
	0.5	$7.6\ 10^{-5}$	0.004	0.68	1910
	0.4	$1.9\ 10^{-5}$	$5\ 10^{-4}$	0.69	1870
PPA second series	5	0.18	2.15	0.61	1380
	3.0	0.15	1.75	0.64	1320
	2.0	$4.8\ 10^{-2}$	0.7	0.66	1250
	0.9	$5.1\ 10^{-3}$	0.22	0.73	1040
	0.6	$2.0\ 10^{-3}$	0.03	0.74	1010
	0.4	$6.2\ 10^{-4}$	0.008	0.76	1020
	0.28	$2.4\ 10^{-4}$	0.003	0.76	1110
	0.13	$1.0\ 10^{-5}$			

Numerical values are: for PANI(CSA)/CA with $p=7.4\%,2.4\%,1.4\%,0.8\%$, $q=0.05,0.40,0.56,0.88$ and $T_0=400$ K,780 K,1640 K,3400 K, for PANI(PPA)/CA with $p=5\%,0.9\%$, $q=0.71,1.89$ and $T_0=5770$ K,13950 K. But this analysis is limited by two points. Firstly, as can be seen in Fig. 5, fits with, and without, the preexponential term are very close, and could be differentiated only at lower temperatures (higher resistances); this will guide further measurements. Secondly, it is not easier to interpret the dependence of q with p than that of γ. Let us recall that the percolation theory gives $q=0.5$ for Mott's three-dimensional (3D) VRH with $\gamma=\frac{1}{4}$.[30] Whether such a prefactor can be invoked in the granular metal theory is also not known.

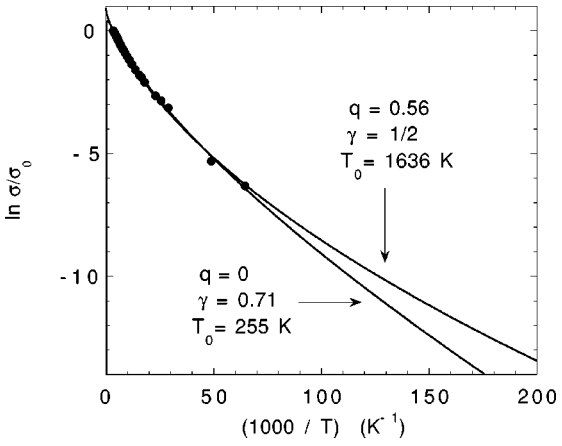

FIG. 5. Comparison of two fitting procedures described by Eqs. (1) and (2) applied to PANI(CSA)/CA with $p=1.4\%$.

C. Magnetoresistance

The influence of a magnetic field B on the low-temperature resistance has been investigated on several samples with CSA and DiOP dopants. Samples with concentration very close to the percolation threshold show a too high resistance for the B dependence to be properly measured. Data for PANI(DiOP)/CA with $p=4\%$ and $T=7.5$ K are plotted in Fig. 6. The quadratic dependence with the field is verified up to the highest B value, 11 T. This is a typical behavior characteristic of all samples of the systems studied. More surprisingly, we found that the coefficient α defined by $\ln(R/R_0)=\alpha B^2$, where $R\equiv R(B)$ and $R_0\equiv R(B=0)$ depends solely on T but neither on the concentration, nor on the type of dopant. The thermal dependence being $\alpha(T)\propto T^{-2}$, we have checked (Fig. 7) that our whole set of data can be represented by a universal function of the parameter B/T.

Chauvet *et al.*[31] have reported on an identical behavior for a series of disordered polypyrroles with various doping levels. Moreover, their points fall on the same universal curve, without any scaling parameter, and the same $(B/T)^2$ dependence. This is recognized as a signature of spin-dependent conduction.

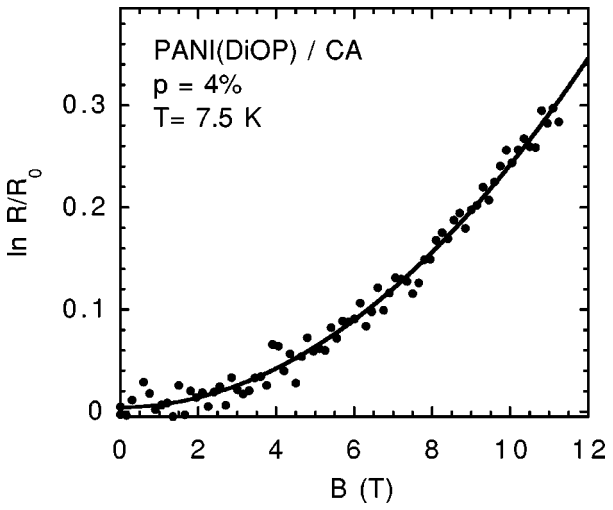

FIG. 6. Magnetoresistance, defined as $\log R/R_0$, of a PANI-DiOP/CA sample with $p=4\%$, measured at $T=7.5$ K. The solid line is a quadratic fit in B.

A model has been recently proposed that takes explicitly into account the spin-flip scattering among inelastic processes.[32] Magnetic impurities are responsible for such scattering (see Sec. III F) the rate of which decreases as $(B/T)^2$. As a consequence the magnetoresistance (MR) has itself the same form. From the experimental data analyzed in Ref. 32 (quasi-1D charge-transfer salt) the prefactor is between 0.1 and 0.2, comparable to our findings (see Fig. 7) and those of Ref. 31.

In Ref. 6, MR has been analyzed within VRH theory. In localized systems, the most common (orbital) effect of the magnetic field is to shrink the electronic wave functions, enhancing the localization and thus the resistance. However, at low field, this is in competition with a delocalization process originating in the weakening of interference of tunneling paths as the magnetic field introduces phase differences. This negative MR is not observed in our case. Nor has it been observed in the experiments of Ref. 6. It seems that only ''metallic'' conducting polymers at very low temperature may exhibit such effects.[4,33,34]

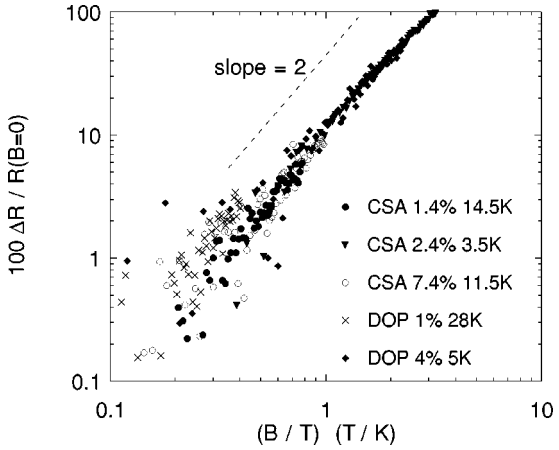

FIG. 7. Universal scaling of the magnetoresistance, defined as $100\Delta R/R_0$ with $\Delta R=R(B)-R(B=0)$, followed by five samples with different dopant and concentration, and at various temperature.

The B^2 dependence of positive MR is predicted by the VRH theory in the intermediate regime with the following expression:[35]

$$\ln(R/R_0)=t\left(\frac{e}{c\hbar}\right)^2 L_c^4\left(\frac{T_0}{T}\right)^{3\gamma}B^2 \tag{3}$$

with $t=0.0035$ when $\gamma=\frac{1}{2}$ and L_c the localization length. In our case, the coefficient of B^2 being proportional to T^{-2} implies that $L_c\propto T^{(3\gamma-2)/4}$, which is a very weak dependence for γ in the range $[\frac{1}{2};\frac{3}{4}]$ (strictly vanishing at $\gamma=\frac{2}{3}$). From Eq. (3) we infer that $L_c\simeq 20$ Å whatever the temperature and concentration, which is quite a reasonable value, interpolating between that of amorphous semiconductors and that of shallow impurities in crystalline semiconductors.[36]

The role of the spin effect in VRH has also been treated.[37] The involved mechanism is the blocking of hopping due to spin polarization. In this model, $\ln R/\ln R_0$ should scale with $(B/k_BT)\ln R$. We have checked that this does not correctly account for our data.

The applicability of VRH to CP is nevertheless controversial.[24,25] In the case of granular materials that we believe may describe our materials (see Sec. III B), the shrinkage effect also occurs and a positive MR is the generic rule. Negative MR seldom occurs, in that case a level crossing origin has been proposed which only takes place for large and close conducting grains.[38]

D. Radio-frequency conductivity

Measurements of ac conductivity at RT and low temperature have been performed mainly on PANI(PPA)/CA samples in the frequency range 10 Hz–1 GHz. For these frequencies and thin films, the conductivity is directly proportional to the admittance. It should be noted that the geometrical coefficient of proportionality is not perfectly known because one of the electrodes is the collet of the APC7 connector. Despite the gold deposit, the 3-mm-diam surface is not equipotential, so that the application of the Marcuvitz formula to a 3-mm-diam lossy capacitor with lateral leakages underestimates the true conductivity. This is a minor drawback because we are mainly interested in conductivity ratios.

RT data for various p are presented in Fig. 8(a). The traditional behavior of disordered conductors is recovered: $\sigma(\omega)$ remains constant at low frequency up to some onset ω_0 where it starts to increase with an approximate power law dependence on ω. Scaling properties are shown in Fig. 8(b) where the same data have been redrawn in reduced units. The conductivity is naturally divided by its $\omega\rightarrow 0$ limit whereas the reduced frequency $\tilde{\omega}\equiv\omega/\omega_0(p)$ is found by trial and error: $\omega_0(p)$ is the numerical factor by which actual frequencies should be divided for data points to collapse on a master curve. This procedure is thus independent on any fitting formula for $\sigma(\omega)$. The fit is performed afterwards and displayed in Fig. 8(b).

The same procedure has been applied to measurements at various T ($24\text{ K}\leqslant T\leqslant 300\text{ K}$) in the case of the $p=0.9\%$ sample for which the onset frequency lies in the experimental frequency range at each temperature. Corresponding data are presented in Fig. 9.

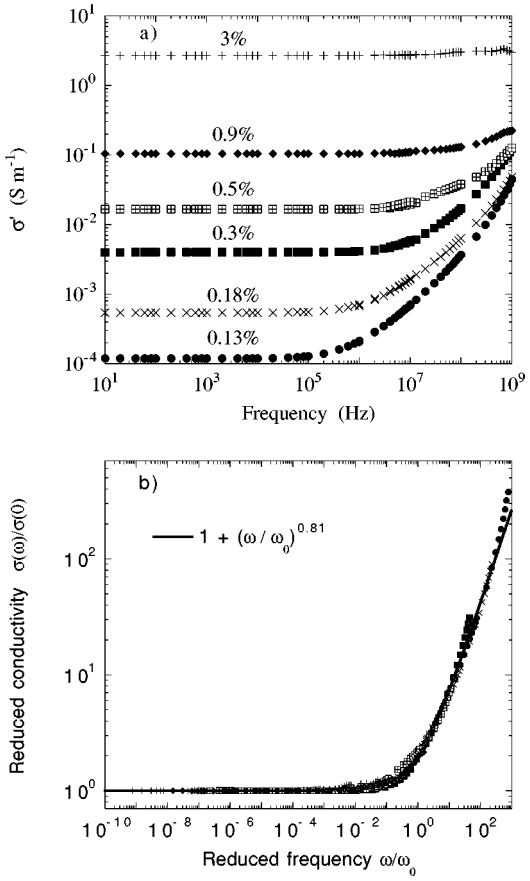

FIG. 8. (a) Frequency dependence of the RT ac conductivity for PANI(PPA)/CA samples with PANI content p ranging from 0.13% to 3%; (b) Same data plotted in reduced units and fitted to the EPA-like scaling law.

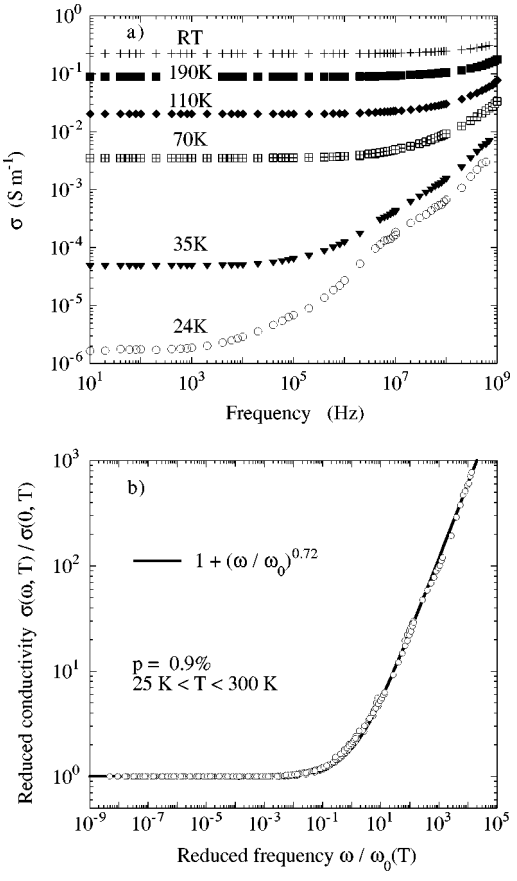

FIG. 9. (a) Frequency dependence of the ac conductivity for PANI(PPA)/CA with $p=0.9\%$ at temperatures ranging from 24 to 300 K; (b) Same data plotted in reduced units and fitted to the EPA-like scaling law.

We claim our data are best represented by the scaling formula

$$\tilde{\sigma}(\omega,p,T)=1+\tilde{\omega}^{u} \tag{4}$$

with

$$\tilde{\sigma}(\omega,p,T)=\frac{\sigma(\omega,p,T)}{\sigma(0,p,T)},$$

$$\tilde{\omega}=\frac{\omega}{\omega_0(p,T)},$$

$$u\in[0.7;0.8].$$

This is the simplest expression containing the two asymptotic behaviors mentioned above, which was previously derived as a general scaling law implied for ac conductivities calculated in the extended pair approximation (EPA) for a variety of models.[39] Moreover, $\omega_0(p,T)$ is found to be closely related to $\sigma(0,p,T)$ as can be seen in Fig. 10. The relationship is nearly that of proportionality whatever the parameter, p or T. It contrasts with the findings of EPA where $\omega_0(T)\propto T\sigma(0,T)$. In the wide class of systems exhibiting the same scaling for $\sigma(\omega,T)$ one can generally relate ω_0 and $\sigma(\omega=0)$ by[40]

$$\omega_0(T)\propto T^{q}\sigma(0,T) \tag{5}$$

with $q=1$ for heavily doped n-type Si and ionic glasses,[41] $q=0.6$ for Au-doped amorphous Si, $q=0$ (our case) for amorphous Si and Ge, carbon black composites,[17] and Pd-based metal cluster compounds,[42] $q=-\frac{1}{4}$ for $2d$ conductor $La_2NiO_{4+\delta}$.[43] According to Hunt[40] this T^q dependence arises from the T^{-q} term in the prefactor of $\sigma(0,T)$ (see Sec. III B) leading to

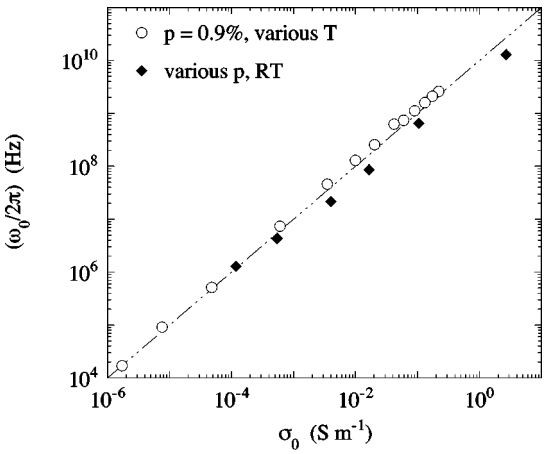

FIG. 10. Correlation between the onset frequency ω_0 and the static conductivity σ_0 for PANI(PPA)/CA samples at various T and p. The dot-dashed line has slope 1.

$$\omega_0(T)=\nu_{\rm ph}\exp\left[-\left(\frac{T_0}{T}\right)^{\gamma}\right].$$

In that sense ω_0 is not system dependent for systems that belong to the same γ-hopping model family. We have seen (Sec. III B) that an alternative description of our data could involve such a prefactor. We do not observe, however, its counterpart in the $\omega_0-\sigma(0)$ relationship.

Let us mention that for one thicker sample ($e=200$ μm), one might accept $q\neq 0$ in Eq. (5). But q remains small $\simeq -0.15$ and we would not claim that this sample significantly departs from the general rule.

It was shown in Sec. III A that $\sigma_{\rm dc}$ was related to percolation phenomena. For the percolation theory, $\omega_0\equiv\omega_\xi$ splits two diffusion regimes: anomalous for $l<\xi$ or $\omega>\omega_\xi$ and normal otherwise. Here l is the typical distance spanned by the charge carrier at frequency ω and ξ the correlation length. ω_ξ and $\sigma(0)$ are therefore related by[44]

$$\sigma(0)\propto(p-p_c)^t,$$

$$\omega_\xi\propto\xi^{-d_w},$$

$$\xi\propto(p-p_c)^{-\nu}$$

with $[d_w=2+(t-\beta/\nu)]$ the walk dimension and β the percolation cluster exponent, thus

$$\omega_\xi\propto\sigma(0)^z \quad \text{with } z=1+\frac{2\nu-\beta}{t}. \tag{6}$$

For the 3D values of universal exponents $\nu=0.88$ and $\beta=0.4$, one finds $z\geqslant 1.5$ in Eq. (6) for $t=2.0$ or 2.3, which is inconsistent with the data of Fig. 10 ($z\simeq 1$).

An alternative description of ac conductivity that tries to go beyond the pair approximation, in order to cross over to the dc limit, has been proposed by Dyre;[45] starting from the same experimental evidence that numerous data seem to appeal for a universal behavior, Dyre derives a scaling law from a general random free-energy barrier model as follows:

$$\tilde{\sigma}=\frac{i\tilde{\omega}}{\ln(1+i\tilde{\omega})}, \tag{7}$$

which proves to be extremely close to the Bryksin equation,[46]

$$\tilde{\sigma}\ln(\tilde{\sigma})=i\tilde{\omega}. \tag{8}$$

In Eq. (7), the scaling factor for $\tilde{\omega}$ is $\Gamma_{\rm min}$, the smallest jump frequency encountered in the system. It is the only parameter except the ''unavoidable'' $\sigma(0)$. As for pair approximation, Eq. (7) is equivalent to $\sigma(\omega)\propto\tilde{\omega}^{0.8}$ for $\tilde{\omega}\gg 1$. Figure 11 shows that Eqs. (4) and (7) gives reasonably good and close fits at least when u in Eq. (4) is not too far from 0.8.

This is not always the case. In Ref. 47, PANI/PE blends, obtained by thermal processing, follow Eq. (4) with $u=0.6$, further from 0.8. We do not know if this has to do with the mesoscopic structure of the blends. In the latter case, they are bulk materials and not films; moreover, due to the quite different process, the state of mixing between conducting and insulating parts obviously differs.

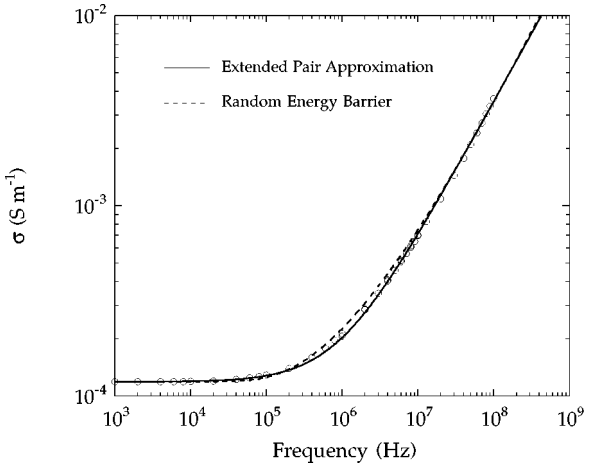

FIG. 11. Comparison of the extended pair approximation and the random free-energy barrier model to the conductivity of PANI(PPA)/CA with $p=0.13\%$.

E. Microwave conductivity

High-frequency complex permittivity ϵ^* has been measured on PANI(CSA)/CA blends for various PANI weight fractions p. For this series, the percolation threshold was found to be around $p_c=0.1\%$ in dc-conductivity measurements. The values at $\nu=\omega/2\pi=5$ GHz are presented on Fig. 12.

At this frequency, the charge carrier follows short paths inside ''clusters'' — what is the exact nature of a cluster in our systems is actually not obvious, see Sec. IV — so that no singularity is expected in the vicinity of p_c on the $\epsilon^*(p)$ curve. We do find a regular increase of ϵ' and ϵ'' with p that can be compared with effective medium calculations.

The permittivity of pure PANI(CSA) cannot be reached in our setup because of its too high value; the reflection coefficient is almost -1, quasi-indistinguishable from that of a ''perfect'' conductor. But using the cavity perturbation tech-

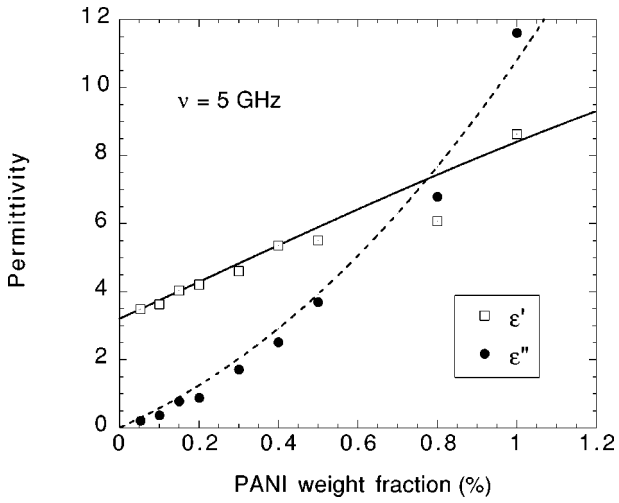

FIG. 12. Complex permittivity (real and imaginary parts) of PANI(CSA)/CA blends at frequency 5 GHz, RT, and for various p. The solid and dashed lines are the real and imaginary parts, respectively, of the permittivity of a mixing calculated by the Lichtenecker formula with $k=0.41$ and component permittivities $\epsilon_{\rm CA}=3.2-j0$, $\epsilon_{\rm PANI}=-6\,10^4-j\sigma_{\rm PANI}/\epsilon_0\omega$ and $\sigma_{\rm PANI}=800$ S cm^{-1}.

nique at the single frequency 6.5 GHz, Joo *et al.*[48] have shown that the same nominal sample [a PANI(CSA) film cast from *m*-cresol] exhibit a metallic behavior with a very high negative real part $\epsilon' = -6\ 10^4$ at RT; here and hereafter ϵ stands for the relative permittivity ϵ_r. The (real) part of conductivity is also greatly enhanced compared to its dc value: $\sigma_{mw} = 6 - 700$ S cm^{-1}

At these very low concentrations, all effective medium approximation (EMA) models derived from the Clausius-Mossotti formula (Maxwell-Garnett, Bruggeman, . . .) have the same (asymptotic) expression and cannot account for the data. In contrast, using values close to those from Ref. 48 in Lichtenecker formula, we get the continous lines of Fig. 12. It reads

$$\epsilon^k_{\text{mixing}} = p\,\epsilon^k_1 + (1-p)\,\epsilon^k_2, \tag{9}$$

where ϵ are the complex values, $\epsilon_1 = \epsilon_{\text{PANI}} = -6\ 10^4 - j\sigma_{\text{PANI}}/\epsilon_0\omega$ with $\sigma_{\text{PANI}} = 800$ S cm^{-1} and $\epsilon_2 = \epsilon_{\text{CA}} = 3.2 - j0$, $j = \sqrt{-1}$, and $k = 0.41$.

Equation (9) is obtained under the mathematical constraint of homogeneity and ''recursivity'' in the sense that it should apply to a mixing of mixings. k is any real number and Eq. (9) reduces to Wiener formulas for $k = \pm 1$, to Loyenga or Landau-Lifshitz for $k = \frac{1}{3}$ and includes the logarithmic one if $x^{k=0}$ stands for ln$x$. Let us mention that $k = \pm 1$ corresponds to serial and parallel arrangements of ''charge'' and ''matrix,'' whereas $k = \frac{1}{3}$ is obtained under the assumption of homogeneous mixing. $k = 0.41$ (found by trial and error) being not too far from $\frac{1}{3}$ allows for some confidence in this description. But with such a high contrast between ϵ_1 and ϵ_2, a small change in k yield a rapid modification of the absolute value of ϵ_{mixing}.

The applicability of EMA to conducting polymers has been recently revisited, for optical frequencies.[49] The CP is considered as a mixture of anisotropic crystalline part embedded in an isotropic amorphous part; Maxwell-Garnett (MG) formalism is applied to this mixture considering a tensorial permittivity ($\epsilon_\perp, \epsilon_\perp, \epsilon_\parallel$) for the crystalline inclusions and a scalar one (ϵ_{host}) for the amorphous host. Because ''host'' and ''inclusion'' are of the same nature (CP) it is natural to define host with the same internal parameters: ϵ_{host} is calculated from two-component EMA with high ($\epsilon_\parallel$) and low ($\epsilon_\perp$) conductivity. It is claimed in Ref. 49 that this model is in a good agreement with PANI or polypyrrole data[50,2] showing a metal-insulator transition. As in any effective medium approximation, it is necessary to consider large ''volume fractions'' to get a nontrivial behavior. Here, two such fractions are considered. For the MG calculation, it is the degree of crystallinity (30–50 %). For the EMA calculation of ϵ_{host}, the authors introduce a measure of disorder f, termed ''connectivity'' of the conducting fibers. There is some critical connectivity (here $f_c = \frac{1}{3}$ for normal 3D EMA) above which ϵ_{mixing} shows a metallic behavior. The introduction of connectivity should be a satisfactory way to image our blends too in some sense; but it is not clear now how to use it for modeling our data as satisfactorily as the Lichtenecker formula does. The step from connectivity f to real weight or volume fraction remains to be found.

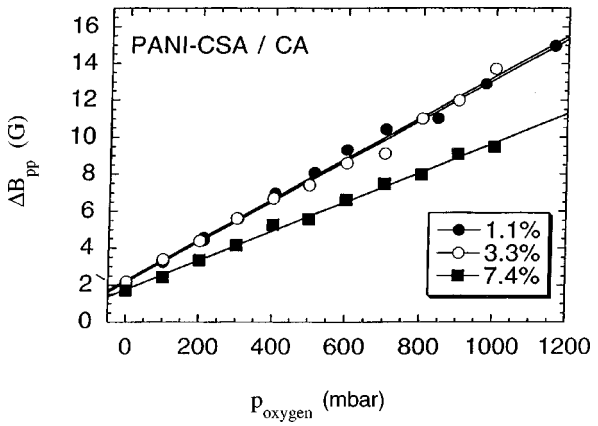

FIG. 13. Evolution of the peak-peak ESR linewidth with the oxygen pressure for different PANI contents in PANI(CSA)/CA blends.

F. ESR

The origin of the ESR linewidth in the case of conducting polymers has been recently revisited.[51] It has been shown that the major source of line broadening is the shortening of the lifetime of the polaron spin state during collisions with fixed spin impurities, even at low spin impurity concentration. In the case of PANI, adsorbed (paramagnetic) molecular oxygen can play the role of fixed spin impurity. Spin flip of polarons while colliding with O_2 happens with high probability (strong exchange regime), so that the line broadening is proportionnal to the polarons hopping frequency ω_{hop}

$$\delta\left(\frac{\Delta B}{\gamma}\right) = p_{\text{sf}}\omega_{\text{hop}}c_{\text{imp}}, \tag{10}$$

where ΔB is the linewidth, γ the gyromagnetic ratio, p_{sf} the spin-flip probability constant, and c_{imp} the impurity concentration. The hopping frequency is a measure of the polaron mobility, and then of the conductivity at microscopic scale: $\omega_{\text{hop}} \propto \sigma_{\text{micro}}$. The major role of polarons in conduction is confirmed by the magnetoresistance results (Sec. III C), which give evidence for a spin-dependent process. In an experiment where c_{imp} is varied, ω_{hop} can be estimated from Eq. (10), which states that, in contrast to conventional motional narrowing and the Elliott mechanism for conduction electrons in metals, the line is broader for more mobile polarons.

We have used this result qualitatively. The ESR linewidth has been measured while monitoring the pressure of O_2. Assuming that c_{imp} is proportional to $p(O_2)$, the amount of ''efficient'' adsorbed oxygen molecules is proportional to the amount of O_2 introduced in the cell. We measured $\Delta B(c_{\text{imp}})$ as a function of $p(O_2)$ for some typical PANI(CSA)/CA samples. Experiments were carried out after stringent drying of samples by long-time secondary pumping; under these conditions the ESR line broadens instantaneously after O_2 pressure application and remains unchanged for hours. The data of linewidth versus $p(O_2)$ are given in Fig. 13 for samples with PANI content from 7.4 to 1.4 %. It appears, from the slopes of the straight lines in Fig. 13, that the microscopic conductivity remains the same, within approximately 30%, while in the same time the dc conductivity var-

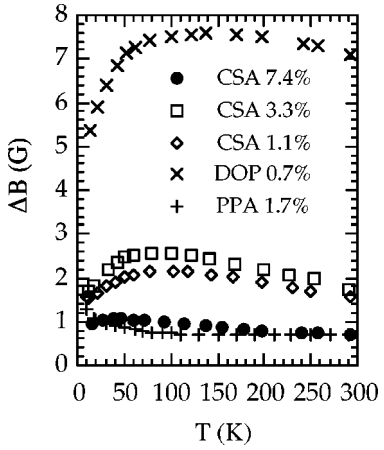

FIG. 14. Evolution of the peak-peak ESR linewidth with temperature for different PANI contents and different dopants in PANI/CA blends.

ies from 2.4 to 1.8×10^{-3} S cm^{-1}. This result is consistent with the picture of a conducting segregated phase, with almost constant intrinsic conductivity.

The temperature dependence of the ESR linewidth has also been measured as a way to determine the temperature dependence of the microscopic conductivity. The samples were placed into tubes, air evacuated and filled with helium for thermal contact. The data are given in Fig. 14 for various samples. They qualitatively behave the same way, except for the PANI(PPA) sample. Namely, $\Delta B(T)$ exhibits a nonmonotonic variation with a maximum value. With the broadening process as described by Eq. (10) a very small amount of fixed spin impurity — typically a few tens of ppm — is sufficient to account for the residual ESR linewidth, i.e., the linewidth observed after pumping. It is likely that such fixed spin impurities can be due to trapped residual molecular oxygen, that cannot be removed by pumping. The different linewidths for the different samples are attributed to different oxygen contaminations. The $\Delta B(T)$ behavior in Fig. 14 is the reverse of the one observed for PANI(HCl) and discussed in a previous work.[52] In Ref. 52 a minimum of ΔB was observed as a function of temperature. The increase of ΔB with increasing T above the minimum was explained in terms of Eq. (10) with a hopping process for the conductivity. The increase of ΔB with decreasing T below the minimum was explained in terms of polaron localization at low temperature. Indeed, the minimum of ΔB originates from the two competing mechanisms. In the present study, the behavior is essentially the opposite: observance of a maximum of $\Delta B(T)$ instead of a minimum. Basically, we explain this difference by the fact that we are dealing with PANI samples doped by dopants that are known to yield highly conducting films. Metallic behavior has been reported in some PANI(CSA) films, namely a negative slope ($d\sigma_{\rm dc}/dT<0$) for T above the temperature of the maximum ($T>T_m$). Below the maximum, ($d\sigma_{\rm dc}/dT>0$) is the signature of a crossover to the hopping regime. It is noteworthy that the ΔB data for PANI(CSA) and PANI(DOP) blends in CA in Fig. 14 reproduce the macroscopic conductivity data ($\sigma_{\rm dc}$) of those films — high-quality 100% PANI films — which exhibit a metallic behavior. We thus explain these ΔB data as reflecting the conductivity at a microscopic scale. The behavior of the PANI(PPA)/CA blend is not understood. We infer that observance of a metallic behavior at a microscopic scale requires less drastic conditions than for the macroscopic scale. The reported values for T_m from $\sigma_{\rm dc}$ measurements are generally beyond 150 K; here T_m is lower than 100 K. Considering that ESR probes all PANI in the sample, whereas $\sigma_{\rm dc}$ is limited by the most resistive regions, this discrepancy does reinforce the heterogeneous image of conducting polymers.

IV. GENERAL DISCUSSION AND CONCLUSION

The challenging question for a global comprehensive description of conducting blend films lies in the quantitative determination of lengthscales for which the dominant transport mechanisms are either macroscopic and relevant to percolation theory, or microscopic and relevant to semiconducting hopping and/or quasi-1D coherent metallic transport.

This question — not yet solved here — also arises because conduction mechanisms in ''pure'' CP are not fully understood. A heterogeneous picture is favored today[5] where the heterogeneity lies in spatially varying characters like doping and crystallinity and its influence is modulated by the amount of disorder. When the strong disorder granular model applies,[25] the characteristic size of heterogeneities is experimentally found to be $d+s\simeq200$ Å, where d is the diameter of the more conducting parts (grain, island, . . .) and s is the typical separation (barrier for hopping). This is found in transport data analysis[24] as well as in structural characterization.[53] TEM micrographs of PANI/PMMA blends[6,18] show that conducting links in the PANI network may be found in the diameter range 100–500 Å, whereas the typical distance between nodes is 400–800 Å. These figures are obtained for $p\geqslant p_c$ but not too far from p_c. When $p\gg p_c$ (a few percent), the system may be described by a 3D arrrangement of PANI ''grains,'' which behaves quite similarly to a pure disordered CP, whence the $\gamma=\frac{1}{2}$ found for $\sigma(T)$. Approaching p_c, the size of the grains is of the same order of that of the links (bundles of PANI chains) which might yield a different behavior: $\gamma>\frac{1}{2}$.

The consideration of actual lengths may be helpful in the understanding of unconventional values of the percolation parameters t and p_c (see Sec. III A). Both are discussed in the two following paragraphs.

From the macroscopic point of view, the system approaching p_c resembles one of the archetypes of continuum percolation: the Swiss-cheese medium, in which the insulating matrix plays the role of large holes. Departure from discrete percolation universality arises when the current has to flow *principally* through narrow ''necks'' with low conductance. It means that the conductivity distribution does not vanish for $\sigma\rightarrow0$. If for instance $g(\sigma)\propto\sigma^{-\alpha},0<\alpha<1$, the transport exponent of percolation is modified to $t'=t+\alpha/(1-\alpha)$ where t is the universal value for lattice percolation.[54] For the Swiss cheese, $\alpha=\frac{1}{3}$ thus $t'_{3d}=2.5$; in our case generally $t'\simeq2.3$, a value also found for other CP blends.[55] Carbon-black/polymer blends also yield nonuniversal exponents.[56] The way such a distribution appears for $p\rightarrow p_c$ is depicted in Fig. 15. The bundles whose diameter does not exceed typical $(d+s)$ values take an increasing importance, so that difficult jumps, those of large s/d, cannot be bypassed.

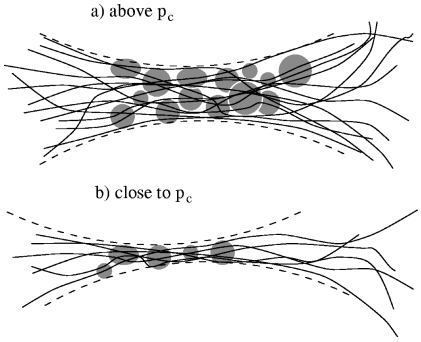

FIG. 15. Schematic view of the narrow ''neck'' concept of continuum percolation applied to PC blends. The dashed lines separate PANI from matrix. Gray domains represent ''grains'' (see definition in the text), whose characteristics don't depend on p. If, approaching p_c, the bundle diameter becomes comparable to typical grain size or separation d and s, the current is no longer able to choose optimal paths — optimal s/d — a necessary condition for $\gamma=\frac{1}{2}$.

Invoking continuum percolation also permits us to give some insight into the origin of the very small value of p_c. For lattice site or bond percolation, p_c depends on the lattice itself. But the critical volume fraction ϕ_c is a dimensional invariant.[57] $\phi_c=p_c f=N_c V$ with f the filling factor of the lattice when each site is occupied by a sphere, N_c the critical concentration of spheres and V the volume of each sphere. This allows one to map continuous systems onto discrete lattice systems (as in the Swiss-cheese case). Strong anisotropy of the conducting object can also be introduced by an (average) excluded volume $V_{\rm ex}$, in which the center of another object cannot be found. It is simply related to the critical number of bonds per site B_c by $B_c=N_c V_{\rm ex}$,[58] which is only shape-characteristic — i.e., independent of size distribution and orientation. Balberg[57] thus wrote the generalized expression $\phi_c=1-\exp(-B_c V/V_{\rm ex})$. It leads to $\phi_c \propto V/V_{\rm ex}$ = radius/length, the aspect ratio, for chains or bundles of chains.

In conclusion our study of several families of PANI/CA conducting blends shows that conduction processes concern many length scales. At the chain scale, ESR and microwave conductivity let intrinsic PANI metallic behavior appear whereas static and low-frequency conductivities reveal the importance of long-range correlations and cluster effects. The spin-dependent nature of conduction also seems to be revealed by magnetoresistance experiments.

Work currently under progress is aimed at improving and extending measurements of electrical properties in the neighborhood of the conduction threshold. It has proved important to ensure precise values for percolation exponents, for low-temperature conductivities and permittivities, in order to discriminate between different formal descriptions. Deeper insight into the mesostructure is needed in the meantime; electron and near-field microscopies will be used for that purpose.

*Electronic address: jplanes@cea.fr

[1] Y. Cao, P. Smith, and A.J. Heeger, Synth. Met. **48**, 91 (1992).
[2] R.S. Kohlman, J. Joo, Y.G. Min, A.G. MacDiarmid, and A.J. Epstein, Phys. Rev. Lett. **77**, 2766 (1996).
[3] R.S. Kohlman, A. Zibold, D.B. Tanner, G.G. Ihas, T. Ishiguro, Y.G. Min, A.G. MacDiarmid, and A.J. Epstein, Phys. Rev. Lett. **78**, 3915 (1997).
[4] M. Ahlskog, M. Reghu and A.J. Heeger, J. Phys.: Condens. Matter **9**, 4145 (1997).
[5] J.P. Travers, J. Chim. Phys. Phys.-Chim. Biol. **95**, 1427 (1998).
[6] M. Reghu, C.O. Yoon, C.Y. Yang, D. Moses, P. Smith, A.J. Heeger, and Y. Cao, Phys. Rev. B **50**, 13 931 (1994).
[7] A. Proń, Y. Nicolau, F. Genoud, and M. Nechtschein, J. Appl. Polym. Sci. **63**, 971 (1997).
[8] P. Rannou, Ph.D. thesis, Université J. Fourier, Grenoble, France, 1998.
[9] B. Wessling, in *Handbook of Conducting Polymers*, 2nd ed., edited by T.A. Skotheim, R.L. Elsenbaumer, and J.R. Reynolds (Marcel Dekker Inc., New York, 1998), pp. 467–530.
[10] B. Sixou, Ph.D. thesis, Université J. Fourier, Grenoble, France, 1996.
[11] B. Sixou and J. P. Travers, J. Phys.: Condens. Matter **10**, 593 (1998).
[12] These values have been still increased since then by use of low-temperature synthesis; see P.M. Beadle, Y.F. Nicolau, E. Banka, P. Rannou, and D. Djurado, Synth. Met. **95**, 29 (1998).
[13] N. Marcuvitz, in *Waveguide Handbook*, 1st ed., edited by N. Marcuvitz (McGraw Hill, New York, 1951), p. 178.
[14] N. Belhadj-Tahar and A. Fourrier-Lamer, IEEE Trans. Microwave Theory Tech. **34**, 346 (1986); R.A. Waldron, in *Theory of Guided Electromagnetic Waves*, edited by R. A. Waldron (Van Nostrand Reinhold Co., London, 1969), pp. 483-493.
[15] A. Fizazi, J. Moulton, K. Pakbaz, S.D.D.V. Rughooputh, P. Smith, and A.J. Heeger, Phys. Rev. Lett. **64**, 2180 (1990).
[16] P. Banerjee and P.M. Mandal, Synth. Met. **74**, 257 (1995).
[17] L.J. Adriaanse, J.A. Reedijk, P.A.A. Teunissen, H.B. Brom, M.A.J. Michels, and J.C.M. Brokken-Zijp, Phys. Rev. Lett. **78**, 1755 (1997).
[18] C.Y. Yang, Y. Cao, Paul Smith, and A.J. Heeger, Synth. Met. **53**, 293 (1993); C.Y. Yang, M. Reghu, A.J. Heeger, and Y. Cao, *ibid.* **79**, 27 (1996).
[19] K. Levon, A. Margolina, and A.Z. Patashinsky, Macromolecules **26**, 4061 (1993).
[20] R. Zallen, in *The Physics of Amorphous Solids* (Wiley, New York, 1983).
[21] H. Tanaka, Phys. Rev. Lett. **76**, 787 (1996).
[22] T. Taniguchi and A. Onuki, Phys. Rev. Lett. **77**, 4910 (1996).
[23] D. van der Putten, J.T. Moonen, H.B. Brom, J.C.M. Brokken-Zijp, and M.A.J. Michels, Phys. Rev. Lett. **69**, 494 (1992).
[24] B. Sixou, N. Mermilliod, and J. P. Travers, Phys. Rev. B **53**, 4509 (1996).
[25] L. Zuppiroli, M.N. Bussac, S. Paschen, O. Chauvet, and L. Forro, Phys. Rev. B **50**, 5196 (1994).
[26] P. Sheng and J. Klafter, Phys. Rev. B **27**, 2583 (1983).
[27] M. Zhou, P. Sheng, L. Chen, and B. Abeles, Philos. Mag. B **65**, 867 (1992).
[28] E. Cuevas, M. Ortuño, and J. Ruiz, Phys. Rev. Lett. **71**, 1871 (1993).
[29] F. Ladieu and M. Sanquer, Ann. Phys. (Paris) **21**, 267 (1996).
[30] L. Friedman and M. Pollak, Philos. Mag. B **38**, 173 (1978).
[31] O. Chauvet, S. Paschen, L. Forro, L. Zuppiroli, P. Bujard, K. Kai, and W. Wernet, Synth. Met. **63**, 115 (1994).

[32] I. Martin and P. Phillips, Phys. Rev. B **56**, 14 883 (1997).
[33] J.C. Clark, G.G. Ihas, M. Reghu, C.O. Yoon, A.J. Heeger and Y. Cao, J. Low Temp. Phys. **101**, 605 (1995).
[34] M. Ahlskog and M. Reghu, J. Phys.: Condens. Matter **10**, 833 (1998).
[35] B.I. Shklovskii and A.L. Efros, in *Electronic Properties of Doped Semiconductors* (Springer, Berlin, 1984).
[36] H. Overhof, Festkoerperprobleme **XVI**, 239 (1976).
[37] Y. Meir, Europhys. Lett. **33**, 471 (1996).
[38] X.R. Wang and X.C. Xie, Europhys. Lett. **38**, 55 (1997).
[39] S. Summerfield, Philos. Mag. B **52**, 9 (1985).
[40] A. Hunt, Philos. Mag. B **64**, 579 (1991).
[41] B. Roling, A. Happe, K. Funke, and M.D. Ingram, Phys. Rev. Lett. **78**, 2160 (1997).
[42] L.J. Adriansee, J.A. Reedijk, H.B. Brom, L.J. de Jongh, and G. Schmid, Z. Phys. D **40**, 123 (1997).
[43] H. Jhans, D. Kim, R.J. Rasmussen, and J.M. Honig, Phys. Rev. B **54**, 11 224 (1996).
[44] S. Havlin and D. Ben-Avraham, Adv. Phys. **36**, 695 (1987).
[45] J.C. Dyre, J. Appl. Phys. **64**, 2456 (1988).
[46] V.V. Bryksin, Fiz. Tverd. Tela (Leningrad) **22**, 2441 (1980) [Sov. Phys. Solid State **22**, 1421 (1980)].
[47] J.P. Yang, P. Rannou, J. Planès, A. Proń, and M. Nechtschein, Synth Met. **93**, 169 (1998).
[48] J. Joo, Z. Oblakovski, G. Du, J.P. Pouget, E.J. Oh, J.M. Wiesinger, Y. Min, A.G. MacDiarmid, and A.J. Epstein, Phys. Rev. B **49**, 2977 (1994).
[49] O. Levy and D. Stroud, Phys. Rev. B **56**, 8035 (1997); J. Phys.: Condens. Matter **9**, L599 (1997).
[50] R.S. Kohlman, J. Joo, Y.Z. Wang, J.P. Pouget, H. Kaneko, T. Ishiguro, and A.J. Epstein, Phys. Rev. Lett. **74**, 773 (1995).
[51] E. Houzé and M. Nechtschein, Phys. Rev. B **53**, 14 309 (1996).
[52] E. Houzé, M. Nechtschein, and A. Proń, Phys. Rev. B **56**, 12 263 (1997).
[53] F. Zuo, M. Angelopoulos, A.G. MacDiarmid, and A.J. Epstein, Phys. Rev. B **36**, 3475 (1987).
[54] S. Feng, B.I. Halperin, and P.N. Sen, Phys. Rev. B **35**, 197 (1987).
[55] B. Sixou, J.P. Travers, C. Barthet, and M. Guglielmi, Phys. Rev. B **56**, 4604 (1997).
[56] I. Balberg, Phys. Rev. Lett. **59**, 1305 (1987).
[57] I. Balberg, Philos. Mag. B **56**, 991 (1987).
[58] This is the same B_c that is used in the percolation treatment of variable range hopping: see V. Ambegaokar, B.I. Halperin, and J.S. Langer, Phys. Rev. B **4**, 2612 (1971).